Pergamon

Int. J. Solids Structures Vol. 35, Nos. 1–2, pp. 129–148, 1998

0020–7683/98 $19.00 + .00

PII: S0020–7683(97)00059–0

MODAL IMPEDANCES FOR A SPHERICAL SOURCE IN A FLUID-FILLED SPHERICAL CAVITY EMBEDDED WITHIN A FLUID-INFILTRATED ELASTIC POROUS MEDIUM

SEYED M. HASHEMINEJAD

Department of Mechanical Engineering, Iran University of Science and Technology, Narmak. Tehran 16844, Iran

(*Received* 25 *January* 1996; *in revised form* 25 *September* 1996)

Abstract—Modal acoustic radiation impedance load on a spherical source vibrating with an arbitrary, axisymmetric, time harmonic velocity distribution, while positioned concentrically within a fluid sphere which is embedded in an infinite fluid-saturated poroelastic medium, is computed. This configuration, which is a realistic idealization of sound projector (transducer) freely suspended in a fluid-filled spherical cavity within a permeable surrounding formation, is of practical importance with a multitude of possible applications in seismo-acoustics and noise control engineering. The formulation utilizes Biot theory of sound propagation in elastic porous media along with the appropriate wave field expansions and the pertinent boundary conditions to determine the resistive and reactive components of model radiation impedances. Numerical example for spherical surface excited in vibrational modes of various order (i.e., monopole, dipole, quadrupole, and multipole like radiators) immersed in a water-filled cavity which is embedded within a water-saturated sandstone surrounding formation is presented. Several limiting cases are discussed. Effects of porosity, frame stiffness, source size and interface permeability condition on the impedance values are presented and discussed. The presented formulation is equally adequate for situations in which the surrounding formation consists of fibrous materials, as in noise control engineering applications. © 1997 Elsevier Science Ltd.

NOTATIONS

$\mathbf{u}$	average macroscopic frame displacement
$\mathbf{U}$	average macroscopic fluid displacement
$\mathbf{w}$	filtration displacement vector
e	average frame dilatation
ε	average fluid dilatation
ξ	increment of fluid content
σ_{ij}	macroscopic stress tensor
e_{ij}	macroscopic strain tensor
p_p	mean pore fluid pressure
λ_f	first Lamé coefficient for a "closed" system (i.e., for $\xi = 0$)
μ	shear modulus of the bare skeletal frame
η	saturating fluid viscosity
ϕ_0	pore volume fraction (porosity)
K_o	bulk modulus of the dry skeleton (i.e., for the "open" system, $p_p = 0$)
K_s	bulk modulus of the material constituting the elastic matrix
K_{fl}	bulk modulus of the saturating fluid
K_f	bulk modulus of the "closed" system
α	tortuosity (infinite frequency)
κ	absolute (dc) permeability of porous medium (zero frequency)
κ_s	characterizes the permeability of the interface
Λ	viscous characteristic length
ω_c	characteristic frequency of the porous medium
ρ	total mass density of the fluid-saturated material
ρ_s	density of the solid matrix material in a consolidated non-porous state
ρ_{fl}	density of the saturating fluid
$\rho_{11}, \rho_{12}, \rho_{22}$	Biot's effective densities
λ, Q, R, M, β	elastic material constants for the solid–liquid aggregate
$\mathbf{s}$	displacement vector of the cavity fluid
p	acoustic pressure in the cavity fluid
c	compressional phase velocity in the cavity fluid
$\bar{\rho}$	density of the cavity fluid.

1. INTRODUCTION

There has been a surpassing interest in the acoustics of fluid-saturated porous media due to its significance in various technical and engineering processes ranging from geophysics, ocean acoustics, architectural acoustics, noise control engineering and tunnel engineering to biophysics and materials engineering. In particular there is an increasing demand to study the propagation of elastic waves in granular media such as rock formations in petroleum reservoirs and ocean bed sedimentary layers, and in fibrous media such as biological tissues, polymer networks, and sound absorbent materials.

In dealing with acoustic problems of poroelastic media one may have to consider various appropriate models. Gassmann (1951) presented the first concise model for harmonic plane wave propagation in an infinite fluid-saturated porous solid. His treatment, however, disregarded the relative viscous fluid/elastic solid motion which is known to be the main cause of energy loss in the high frequency regime. Biot (1956a, b) approached the problem in a more unified manner and formulated the appropriate constitutive equations and equations of motion in poroelastic media. He predicted the existence of two types of dilatational (compressional) waves along with one rotational (shear) wave. Biot's treatment agrees with Gassmann's results in the low frequency range (White, 1983). Geertsma and Smit (1961) and Deresiewicz and Rice (1962) employed Biot's complete dynamic equations to study the plane interface wave reflection problems.

Recently the scientific groundwork for Biot's model is more firmly established through several experimental validations leading to a renewed interest in the subject. The first experimental observation of the fast and slow bulk waves (as predicted by Biot's theory) was reported by Plona (1980). Subsequently, Berryman (1980) analyzed and confirmed Plona's observations and concluded that the Biot's theory is a satisfactory model of wave speeds and attenuation in poroelastic media.

The appropriate set of boundary conditions which should be satisfied when an interface separates two poroelastic media was derived by Deresiewicz and Skalak (1963). Many researchers have employed these conditions to produce the solution to Biot's equations of motion for various scattering problems. While most of the investigations involve reflection and transmission from a planar interface, comparatively little work has been done on acoustic scattering or radiation from convex-shaped inclusions which is of prominent importance in engineering and geophysics. By applying a boundary layer approximation Mie *et al.* (1984) studied acoustic scattering by a fluid-filled circular cavity within a fluid-infiltrated poroelastic medium. Berryman (1985) and Zimmerman (1993) have each employed different analytical methods to examine scattering of plane compressional waves by a spherical inclusion in an infinite poroelastic medium. In a later study, Kargl and Lim (1993) formulated the scattering problem using a T-matrix approach.

Problems corresponding to sources immersed near a permeable interface are of great practical importance with a multitude of possible applications in technical fields such as seismic prospecting, reservoir seismics, ocean seismo-acoustics, noise control engineering, and hydrology. Noting that most sound projector devices employed in seismo-acoustics are generally of the expander or shaker type, a spherical source is naturally useful as a simplified model of such transducers with roughly the same dimensions. Employing this idealization, Poterasu (1993) investigated dynamic coupling effects for a pulsating source in a fluid-filled cavity embedded within an *elastic* infinite media by the boundary element method. In doing this, however, he made the unrealistic assumption for the surrounding formation to be nonporous and nonpermeable.

The fluctuating acoustic pressure on the surface of a vibrating structure constitutes its radiation loading. The radiation loading on a spherical surface excited in vibrational modes of various orders (i.e., monopole, dipole, quadrupole, and multipole like radiators) is best described through its acoustic radiation impedance. For an excellent review on this subject, and presentation of modal acoustic impedance curves for a spherical source immersed in an unbounded ideal compressible fluid, one should consider Junger and Feit (1972).

The present effort studies radiation loading on a spherical sound projector (transducer) freely suspended in a fluid-filled spherical cavity embedded within a permeable surrounding

formation consisting of fluid-infiltrated elastic porous solid. One very closely related problem of interest, which can readily benefit from present study, is to investigate the vibratory characteristics of the submerged transducer clamped to the cavity wall (see White, 1983, p. 230). The behaviour of such a system is similar to that of a vibrator on a halfspace, in that the mathematical analysis should incorporate the effects of vibrator and fluid inertia, radiation and material damping, and cavity surface and vibrator compliance. For a good demonstration on such analysis the reader is referred to Geers and Hasheminejad (1991). Section 2 contains the governing equations of poroelasticity and the dispersion expressions for phase velocities. In Section 3 the problem and the appropriate boundary conditions are stated and the solution technique presented by Pao and Mow (1973), which involves the solution of a truncated set of algebraic equations, is employed to obtained the impedance relation. Finally, Section 4 discusses numerical implementation and results for the example of a water-filled cavity in a water-saturated sandstone media and some limiting cases.

2. GOVERNING FIELD EQUATIONS

Before proceeding to analyze the full problem, we shall first briefly review highlights of Biot's theory of poroelasticity. A re-examination of the main hypotheses of Biot's model is unnecessary and the reader is directed to standard references on the subject (see, for example, Allard, 1993, Bourbie *et al.*, 1987). Denoting the average macroscopic displacement of the solid frame and the saturating fluid on the elementary macroscopic volume (EMV) by the vectors $\mathbf{u}$ and $\mathbf{U}$, respectively, the macroscopic stress tensor σ_{ij} and the mean pore fluid pressure p_p are defined by (Bourbie *et al.*, 1987)

$$\begin{aligned} \sigma_{ij} &= (\lambda_f e - \beta M \xi)\delta_{ij} + 2\mu e_{ij} \\ p_p &= M(\xi - \beta e) \end{aligned} \tag{1}$$

where

$$\begin{aligned} \lambda_f &= K_f - \tfrac{2}{3}\mu \\ K_f &= \frac{\phi_0(1/K_s - 1/K_{fl}) + 1/K_s - 1/K_o}{\phi_0/K_o(1/K_s - 1/K_{fl}) + 1/K_s(1/K_s - 1/K_o)} \\ M &= 1/((\beta - \phi_0)/K_s + \phi_0/K_{fl}) \\ \beta &= 1 - K_o/K_s \\ e_{ij} &= (u_{i,j} + u_{j,i})/2 \\ \xi &= -\nabla \cdot \mathbf{w} = -\phi_0(\varepsilon - e) \\ e &= \nabla \cdot \mathbf{u}, \quad \varepsilon = \nabla \cdot \mathbf{U} \end{aligned} \tag{2}$$

in which $\mathbf{w} = \phi_0(\mathbf{U} - \mathbf{u})$ is the filtration displacement vector, and a brief description for the important parameters involved in this work is given at the beginning of the paper.

The equations of motion governing the displacements of the solid matrix and interstitial liquid with dissipation taken into account are (Bourbie *et al.* 1987)

$$\begin{aligned} (\lambda + 2\mu)\nabla\nabla \cdot \mathbf{u} + Q\nabla\nabla \cdot \mathbf{U} - \mu\nabla \times \nabla \times \mathbf{u} &= \rho_{11}\ddot{\mathbf{u}} + \rho_{12}\ddot{\mathbf{U}} + b(\dot{\mathbf{u}} - \dot{\mathbf{U}}) \\ Q\nabla\nabla \cdot \mathbf{u} + R\nabla\nabla \cdot \mathbf{U} &= \rho_{12}\ddot{\mathbf{u}} + \rho_{22}\ddot{\mathbf{U}} - b(\dot{\mathbf{u}} - \dot{\mathbf{U}}) \end{aligned} \tag{3}$$

where

$$\begin{aligned} \lambda &= \lambda_f + \phi_0 M(\phi_0 - 2\beta) & \rho &= (1-\phi_0)\rho_s + \phi_0\rho_{fl} \\ Q &= \phi_0 M(\beta - \phi_0) & \rho_{11} &= \rho + \phi_0\rho_{fl}(\alpha - 2) \\ R &= \phi_0^2 M & \rho_{12} &= \phi_0\rho_{fl}(1-\alpha) \\ & & \rho_{22} &= \rho - \rho_{11} - 2\rho_{12} = \alpha\phi_0\rho_{fl} \end{aligned} \tag{4}$$

where the parameter b, which is the viscous friction coefficient due to the relative fluid/solid motion, is given as (Allard, 1993)

$$b = \frac{\phi_0^2 \eta}{\kappa} F(\omega). \tag{5}$$

The quantity $F(\omega)$ is a viscosity correction factor which allows for the fact that effective damping changes when the viscous skin depth $\sqrt{2\eta/\rho_{fl}\omega}$ becomes smaller than the pore size as the frequency increases beyond the characteristic frequency $\omega_c = \phi_0\eta/\rho_{fl}\kappa\alpha$. Many researchers have investigated the frequency dependence of Biot theory in terms of a frequency-dependent dynamic permeability/tortuosity. The interested reader is referred to Johnson *et al.* (1994a) for a recent review. A very simple and fairly accurate model for description of dynamic permeability is proposed by Johnson *et al.* (1987). Their equation (3.3) states

$$F(\omega) = \left\{1 - j\frac{4\alpha^2\kappa^2\rho_{fl}\omega}{\eta\Lambda^2\phi_0^2}\right\}^{1/2} \tag{6}$$

where $\Lambda \approx \sqrt{8\alpha\kappa/\phi_0}$ (Allard, 1993, Winkler *et al.*, 1989) is a viscous characteristic length which depends only on frame geometry and describes the sizes of dynamically connected pores. Hereafter we shall assume harmonic time variations with $e^{-j\omega t}$ dependence suppressed for simplicity. Note that energy dissipation in the solid frame may also be readily incorporated in Biot's model by replacing the solid elastic parameters by appropriate complex functions (Cremer, 1990).

Helmholtz decomposition theorem allows us to resolve the displacement fields as superposition of longitudinal and transverse vector components

$$\begin{aligned} \mathbf{u} &= \nabla\phi + \nabla\times\psi \\ \mathbf{U} &= \nabla\chi + \nabla\times\Theta. \end{aligned} \tag{7}$$

Substituting the above resolutions into Biots' field equations of motion (3), we obtain two sets of coupled equations:

$$\begin{bmatrix} \lambda+2\mu & Q \\ Q & R \end{bmatrix}\begin{bmatrix} \nabla^2\phi \\ \nabla^2\chi \end{bmatrix} = \begin{bmatrix} \rho_{11}\omega^2 - j\omega b & \rho_{12}\omega^2 + j\omega b \\ \rho_{12}\omega^2 + j\omega b & \rho_{22}\omega^2 - j\omega b \end{bmatrix}\begin{bmatrix} \phi \\ \chi \end{bmatrix} \tag{8}$$

$$\begin{bmatrix} \mu & 0 \\ 0 & 0 \end{bmatrix}\begin{bmatrix} \nabla^2\psi \\ 0 \end{bmatrix} = \begin{bmatrix} \rho_{11}\omega^2 - j\omega b & \rho_{12}\omega^2 + j\omega b \\ \rho_{12}\omega^2 + j\omega b & \rho_{22}\omega^2 - j\omega b \end{bmatrix}\begin{bmatrix} \psi \\ \Theta \end{bmatrix}. \tag{9}$$

The above systems may be manipulated to yield Helmholtz equations (Bourbie *et al.* 1987):

$$\begin{aligned} \nabla^2\phi_{f,s} + k_{f,s}^2\phi_{f,s} &= 0 \\ \nabla^2\psi + k_t^2\psi &= 0 \end{aligned} \tag{10}$$

where k_f, k_s, and k_t which designate the complex wave numbers of the fast compressional, slow compressional, and the elastic shear waves, respectively, are given as

$$k_{f,s}^2 = \frac{B \mp \sqrt{B^2 - 4AC}}{2A} \quad k_t^2 = \frac{C}{\mu(\rho_{22}\omega^2 + j\omega b)} \tag{11}$$

where

$$\begin{aligned} A &= (\lambda + 2\mu)R - Q^2 \\ B &= \omega^2[\rho_{11}R + \rho_{22}(\lambda + 2\mu) - 2\rho_{12}Q] + j\omega b(\lambda + 2\mu + 2Q + R) \\ C &= \omega^2[\omega^2(\rho_{11}\rho_{22} - \rho_{12}^2) + j\omega\rho b]. \end{aligned} \tag{12}$$

Employing eqns (8)–(11), with some manipulations, the scalar potentials ϕ, χ, Θ, and ψ may be expressed as

$$\begin{aligned} \phi &= \phi_f + \phi_s \\ \chi &= \mu_f\phi_f + \mu_s\phi_s \\ \Theta &= \alpha_0\psi \end{aligned} \tag{13}$$

where

$$\begin{aligned} \mu_{f,s} &= \frac{\omega^2(\rho_{11}R - \rho_{12}Q) - k_{f,s}^2[(\lambda + 2\mu)R - Q^2] + j\omega b(Q + R)}{\omega^2(\rho_{22}Q - \rho_{12}R) + j\omega b(Q + R)} \\ \alpha_0 &= -\frac{\omega^2\rho_{12} - j\omega b}{\omega^2\rho_{22} + j\omega b}. \end{aligned} \tag{14}$$

The above review clearly points to the existence of three distinct modes of elastic wave propagation in fluid-saturated porous-elastic medium: a predominantly frame-borne fast wave which is coupled with a predominantly fluid-borne slow wave, along with one frame-borne shear wave which is decoupled from the other two modes.

The fluid contained in the spherical cavity is assumed to be inviscid and ideal compressible that cannot support shear stresses making the state of stress in the fluid purely hydrostatic. Consequently the field equations may be expressed in terms of the velocity potential of the cavity fluid as (Achenbach, 1976)

$$\begin{aligned} \dot{\mathbf{s}} &= \nabla\varphi \\ p &= -\bar{\rho}\dot{\varphi} \\ \nabla^2\varphi + k^2\varphi &= 0 \end{aligned} \tag{15}$$

where $k(=\omega/c)$ is the wave number for the dilatational wave, $\bar{\rho}$ is the density, $\dot{\mathbf{s}}$ is the velocity vector, and p is the acoustic pressure in the inviscid fluid.

3. FIELD EXPANSIONS AND BOUNDARY CONDITIONS

The geometry and the coordinate system used are shown in Fig. 1. The problem can be analyzed by means of the standard methods of the theory of mechanical vibrations. The dynamics of the problem may be expressed in terms of four scalar potentials: one corresponds to the compressional wave trapped in the inviscid fluid layer inside the spherical cavity, the other three correspond to the transmitted fast and slow dilatational waves and the transmitted shear wave which propagate outward into the infinite poroelastic medium. Each of these waves can be represented in form of an infinite series whose unknown coefficients are determined by imposing the proper boundary conditions.

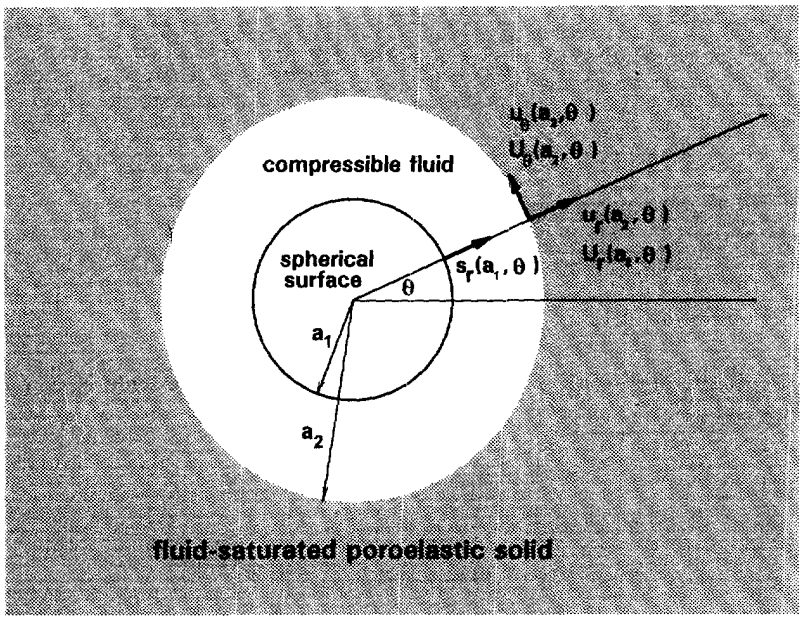

Fig. 1. Problem geometry.

Following our discussion on Helmholtz decomposition in preceding section, the compressional waves which are contained in the interior of the spherical cavity may be expressed as

$$\varphi = \sum_{n=0}^{\infty} [D_n j_n(kr) + E_n h_n(kr)] P_n(\cos\theta) \tag{16}$$

where j_n are spherical Bessel functions, h_n are the spherical Hankel functions, P_n are the Legendre polynomials (Abramovitz and Stegun, 1964), D_n and E_n are unknown scattering coefficients. Similarly, the outgoing transmitted waves in the poroelastic medium exterior to the cavity are expressed as

$$\phi_f = \sum_{n=0}^{\infty} A_n h_n(k_f r) P_n(\cos\theta)$$

$$\phi_s = \sum_{n=0}^{\infty} B_n h_n(k_s r) P_n(\cos\theta)$$

$$\psi = \sum_{n=0}^{\infty} C_n h_n(k_t r) P_n^1(\cos\theta) \tag{17}$$

where $P_n^1(\cos\theta)[= -(\mathrm{d}/\mathrm{d}\theta)P_n(\cos\theta)]$ is the Legendre function.

Now considering the basic field equations in spherical coordinates with axial symmetry (i.e., assuming no azimuthal dependence) the solid and liquid displacements in r- and θ-directions in terms of displacement potentials in the poroelastic media are (Achenbach, 1976)

$$u_r = \frac{\partial\phi}{\partial r} + \frac{1}{r}\frac{\partial\psi}{\partial\theta} + \frac{\psi}{r}\operatorname{ctan}\theta \quad u_\theta = \frac{1}{r}\frac{\partial\phi}{\partial\theta} - \frac{\partial\psi}{\partial r} - \frac{\psi}{r}$$

$$U_r = \frac{\partial\chi}{\partial r} + \frac{1}{r}\frac{\partial\Theta}{\partial\theta} + \frac{\Theta}{r}\operatorname{ctan}\theta \quad U_\theta = \frac{1}{r}\frac{\partial\chi}{\partial\theta} - \frac{\partial\Theta}{\partial r} - \frac{\Theta}{r}. \tag{18}$$

Expressions for the frame and liquid dilatations can be manipulated to yield

$$e = \nabla \cdot \mathbf{u} = \nabla^2 \phi = \nabla^2 \phi_f + \nabla^2 \phi_s = -k_f^2 \phi_f - k_s^2 \phi_s$$
$$\varepsilon = \nabla \cdot \mathbf{U} = \nabla^2 \chi = \mu_f \nabla^2 \phi_f + \mu_s \nabla^2 \phi_s = -\mu_f k_f^2 \phi_f - \mu_s k_s^2 \phi_s \tag{19}$$

where

$$\nabla^2 = \frac{1}{r^2}\frac{\partial}{\partial r}\left(r^2 \frac{\partial}{\partial r}\right) + \frac{1}{r^2 \sin\theta}\frac{\partial}{\partial \theta}\left(\sin\theta \frac{\partial}{\partial \theta}\right). \tag{20}$$

Utilizing (1), (13), (18), and (19), pore fluid pressure, radial and tangential stress components are written as

$$\sigma_{rr} = a_f k_f^2 \phi_f + a_s k_s^2 \phi_s + 2\mu(\partial u_r/\partial r) \tag{21}$$

$$p_p = M b_f k_f^2 \phi_f + M b_s k_s^2 \phi_s \tag{22}$$

$$\sigma_{r\theta} = \frac{\mu}{r}\left(\frac{\partial u_r}{\partial \theta} + r\frac{\partial u_\theta}{\partial r} - u_\theta\right) \tag{23}$$

where

$$a_{f,s} = -\lambda_f + \phi_0 \beta M(1 - \mu_{f,s})$$
$$b_{f,s} = \beta + \phi_0(\mu_{f,s} - 1). \tag{24}$$

The boundary condition at the spherical surface (i.e., at $r = a_1$) is the continuity of normal velocity, thus first of eqn (15) and eqn (16) yield

$$\left.\frac{\partial \varphi}{\partial r}\right]_{r=a_1} = v = \sum_{n=0}^{\infty} v_n P_n(\cos\theta) \tag{25}$$

where v_n represents the modal radial velocity amplitude of the spherical surface (see Fig. 1).

The appropriate boundary conditions which have to be satisfied at the cavity wall (i.e., at $r = a_2$) to yield a unique solution of proposed problem are (Deresiewicz and Skalak, 1963, Bourbie *et al.*, 1987):

(1) Compatibility of normal stress in poroelastic media with the acoustic pressure in the cavity fluid

$$\sigma_{rr} = -p \tag{26a}$$

(2) Vanishing of tangential stress

$$\sigma_{r\theta} = 0 \tag{26b}$$

(3) Continuity of normal component of the filtration velocity

$$\dot{w}_r = \phi_0(\dot{U}_r - \dot{u}_r) = \dot{s}_r - \dot{u}_r \tag{26c}$$

(4) Consistency of the pressure drop and the normal component of filtration velocity (i.e., satisfaction of Darcy's law which governs the fluid flow across the interface)

$$\dot{w}_r = -\kappa_s(p-p_p) \tag{26d}$$

where the parameter κ_s characterizes the permeability of the interface, i.e., the quality of interconnection between two media. For an open interface, we expect zero pressure drop ($p = p_p$) and hence we let $\kappa_s = \infty$. To characterize a sealed interface (i.e., for $\dot{\mathbf{w}} = 0$) we take $\kappa_s = 0$.

Finally, the unknown scattering coefficients shall be determined by imposing the stated boundary conditions. Employing expansions (16) and (17) in the field eqns (18)–(24), and substituting obtained results into the boundary conditions (25) and (26), we acquire

$$kj_n'(ka_1)D_n + kh_n'(ka_1)E_n = v_n \tag{27}$$

$$\{k_f^2[a_f h_n(k_f a_2) + 2\mu h_n''(k_f a_2)]\}A_n + \{k_s^2[a_s h_n(k_s a_2) + 2\mu h_n''(k_s a_2)]\}B_n + \left\{\frac{2\mu n(n+1)}{a_2}\left[k_t h_n'(k_t a_2) - \frac{1}{a_2}h_n(k_t a_2)\right]\right\}C_n + \{j\omega\bar{\rho}j_n(ka_2)\}D_n + \{j\omega\bar{\rho}h_n(ka_2)\}E_n = 0 \tag{28}$$

$$\left\{\frac{2\mu}{a_2}\left[\frac{1}{a_2}h_n(k_f a_2) - k_f h_n'(k_f a_2)\right]\right\}A_n + \left\{\frac{2\mu}{a_2}\left[\frac{1}{a_2}h_n(k_s a_2) - k_s h_n'(k_s a_2)\right]\right\}B_n + \frac{\mu}{a_2^2}\{[2-n(n+1)]h_n(k_t a_2) - a_2^2 k_t^2 h_n''(k_t a_2)\}C_n = 0 \tag{29}$$

$$\{j\omega k_f h_n'(k_f a_2)[\phi_0(1-\mu_f)-1]\}A_n + \{j\omega k_s h_n'(k_s a_2)[\phi_0(1-\mu_s)-1]\}B_n + \left\{\frac{n(n+1)}{a_2}j\omega h_n(k_t a_2)[\phi_0(1-\alpha_0)-1]\right\}C_n + \{-kj_n'(ka_2)\}D_n + \{-kh_n'(ka_2)\}E_n = 0 \tag{30}$$

$$\{j\omega\phi_0 k_f h_n'(k_f a_2)[1-\mu_f] - \kappa_s M b_f k_f^2 h_n(k_f a_2)\}A_n + \{j\omega\phi_0 k_s h_n'(k_s a_2)[1-\mu_s] - \kappa_s M b_s k_s^2 h_n(k_s a_2)\}B_n + \left\{\frac{n(n+1)}{a_2}j\omega\phi_0 h_n(k_t a_2)[1-\alpha_0]\right\}C_n + \{j\omega\bar{\rho}\kappa_s j_n(ka_2)\}D_n + \{j\omega\bar{\rho}\kappa_s h_n(ka_2)\}E_n = 0 \tag{31}$$

where $n = 0, 1, 2, \ldots$, except for eqn (29) where $n = 1, 2, \ldots$.

The system of eqns (27)–(31) may beneficially be put in matrix form as

$$\mathbf{u}_0 = \mathbf{R}_0\mathbf{c}_0, \quad \mathbf{u}_n = \mathbf{R}_n\mathbf{c}_n \quad n \geqslant 1 \tag{32}$$

where

$$\mathbf{c}_0 = [A_0, B_0, D_0, E_0]^{\mathrm{T}} \quad \mathbf{c}_n = [A_n, B_n, C_n, D_n, E_n]^{\mathrm{T}}$$
$$\mathbf{u}_0 = [v_0, 0, 0, 0]^{\mathrm{T}} \quad \mathbf{u}_n = [v_n, 0, 0, 0, 0]^{\mathrm{T}}. \tag{33}$$

Fluid pressure on the vibrating spherical surface is determined from second of eqn (15) and eqn (16) as

$$p_n(r = a_1) = \{j\omega\bar{\rho}j_n(ka_1)\}D_n + \{j\omega\bar{\rho}h_n(ka_1)\}E_n \tag{34}$$

which can readily be put in matrix form as

$$p_0 = \mathbf{S}_0\mathbf{c}_0, \quad p_n = \mathbf{S}_n\mathbf{c}_n \quad n \geqslant 1. \tag{35}$$

Using eqns (32) and (35), modal pressure may be stated as

$$p_0 = \mathbf{Z}_0\mathbf{u}_0, \quad p_n = \mathbf{Z}_n\mathbf{u}_n \quad n \geqslant 1 \tag{36}$$

where

$$\mathbf{Z}_0 = \mathbf{S}_0\mathbf{R}_0^{-1}, \quad \mathbf{Z}_n = \mathbf{S}_n\mathbf{R}_n^{-1} \quad n \geqslant 1. \tag{37}$$

Finally, noting the structure of the vectors $\mathbf{u}_0$ and $\mathbf{u}_n$, we identify the acoustic impedance for modal vibrations of the spherical surface inside the cavity, z_n, as the first element of the "**Z**" matrix (see Hasheminejad and Geers, 1993). Moreover, modal acoustic impedance can be expressed in terms of its resistive and reactive components as (see Junger and Feit, 1972)

$$z_n(\omega) = \tilde{\rho}cr_n(\omega) - i\omega\tilde{\rho}a_1 m_n(\omega). \tag{38}$$

4. NUMERICAL RESULTS

In order to illustrate the nature and behaviour of the solution, we consider a numerical example in this section. Realizing the large number of parameters involved here, no attempt is made to exhaustively evaluate the effect of varying each of them. The intent of the collection of data presented here is merely to illustrate the kinds of results to be expected from some representative and physically realistic choices of values for these parameters. From these data some trends are noted and general conclusions made about the relative importance of certain parameters. A FORTRAN program for computing $\mathbf{Z} = \mathbf{S}\mathbf{R}^{-1}$ was constructed to calculate modal acoustic impedance values as functions of $ka_1 = \omega a_1/c$. Accurate computations of spherical Bessel functions of complex argument were performed with the subroutine SBESJH (Thompson and Barnett, 1987); their derivatives were computed by utilizing (10.1.19) and (10.1.22) in Abramovitz and Stegun (1964). All computations were performed in double precision on a Sun-Spark Classic workstation.

Noting the crowd of parameters which enter into the final expressions and keeping in view the availability of numerical data, we shall confine our attention to a particular model. Johnson *et al.* (1994b) have experimentally determined the required input parameters to calculate the basic acoustic properties of water-saturated Ridgefield Sandstone within the context of Biot theory. These input parameter values, which are used in the calculations, are compiled in Table 1.

Table 1. Input parameter values in Biot's model

Parameter	Water-saturated sandstone
ϕ_0	0.37
α	1.58
κ (cm^2)	27.7×10^{-8}
ρ_s (g/cm^3)	2.48
K_s (dyn/cm^2)	4.99×10^{11}
K_o (dyn/cm^2)	5.24×10^{10}
μ (dyn/cm^2)	3.26×10^{10}
ρ_{fl} (g/cm^3)	1.00
K_{fl} (dyn/cm^2)	2.25×10^{10}
η (g/cm · sec)	0.01
Λ (cm)	19.4×10^{-4}
$\omega_c/2\pi$ (kHz) [calculated]	1.33

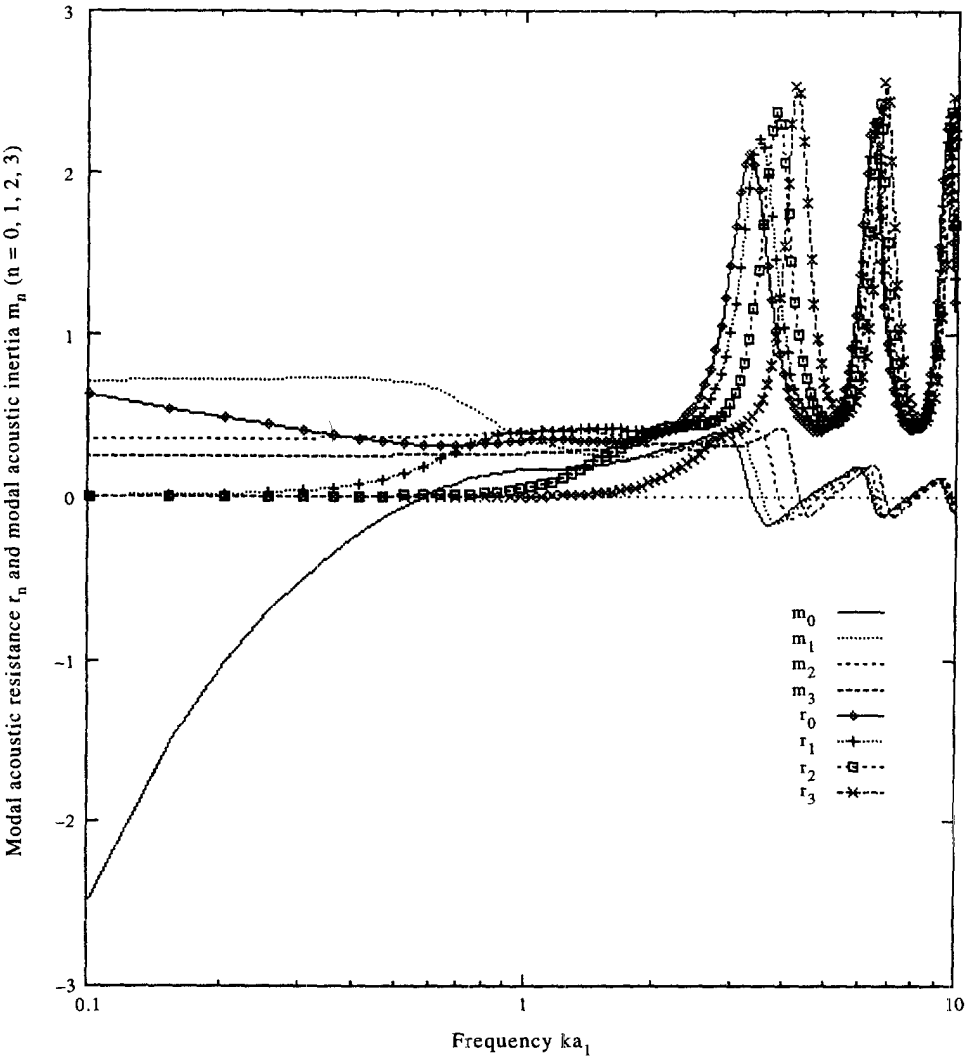

Fig. 2. Modal acoustic impedance curves for $a_2/a_1 = 20$ cm/10 cm ($\kappa_s = \infty$, $\omega_c a_1/c = 0.56$, other parameters as in Table 1).

Figures 2 and 3 each displays the inertial and the resistive components of the modal acoustic impedance, for a radii ratio of $a_2/a_1 = 20$ cm/10 cm, and 200 cm/100 cm, respectively, with open interface condition (i.e., $\kappa_s = \infty$) and basic material properties as given in Table 1. Here we note the high frequency oscillations of modal impedance curves which is due to boundary interference and reveberation effects, as is discussed in detail by Hasheminejad and Geers (1992).

Several computer program runs were made using various source and cavity sizes in order to assess the effects of interface condition, porosity, and frame stiffness on modal impedance results. It was concluded that the most pronounced overall effects occur for a radii ratio near unity (i.e., small gap size). Figures 4–6 display such effects for the selected radii ratio of $a_2/a_1 = 12$ cm/10 cm. The effect of interface condition on modal impedance may be studied through the parameter $0 \leqslant \kappa_s < \infty$ which as explained before characterizes the permeability of the interface. For simplicity we have only considered two limiting cases of $\kappa_s = \infty$ (fully open interface) and $\kappa_s = 0$ (completely sealed interface). The relevant results are compared in Figs 4a and 4b. As expected, the modal impedance values increase as the quality of interconnection weakens. Note the extremely high reactance value obtained for the $n = 0$ ("breathing") mode in the sealed interface case (i.e., $m_0 = -180.64@ka_1 = 0.1$).

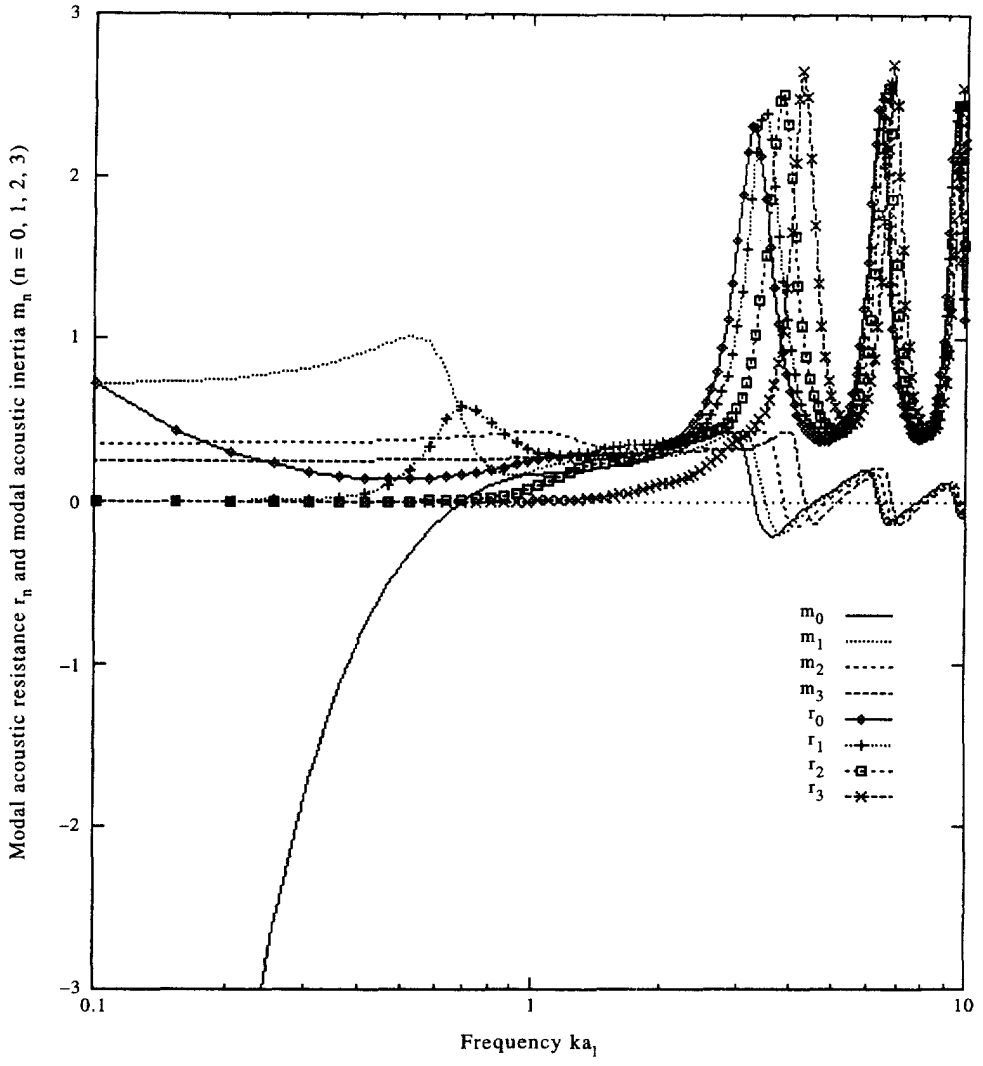

Fig. 3. Modal acoustic impedance curves for $a_2/a_1 = 200$ cm/100 cm ($\kappa_s = \infty$, $\omega_c a_1/c = 5.57$, other parameters as in Table 1; $m_0 = -15.71 @ ka_1 = 0.1$).

The influence of porosity on modal impedance curves is shown in Figs 5a and 5b. For the reason of clarity only two porosity values are examined, namely $\phi_0 = 0.27$ and $\phi_0 = 0.47$. The related tortuosity and Λ values are obtained by scaling the experimental values given in Table 1 according to the following approximations

$$\alpha \approx 1/\sqrt{\phi_0} \quad \text{(Berryman, 1982)}$$
$$\Lambda \approx \sqrt{8\alpha\kappa/\phi_0} \quad \text{(Winkler } et\ al.\text{, 1989).} \tag{39}$$

Table 2 displays the input parameter values for α, and Λ which are utilized in numerical

Table 2. Estimated values for tortousity, characteristic viscous length and frequency (note: values listed in the first row are experimental, taken from Table 1)

ϕ_0	α	Λ	ω_c
0.37	1.58	19.4×10^{-4}	8.36×10^3
0.27	1.85	24.7×10^{-4}	5.18×10^3
0.47	1.40	16.2×10^{-4}	12.02×10^3

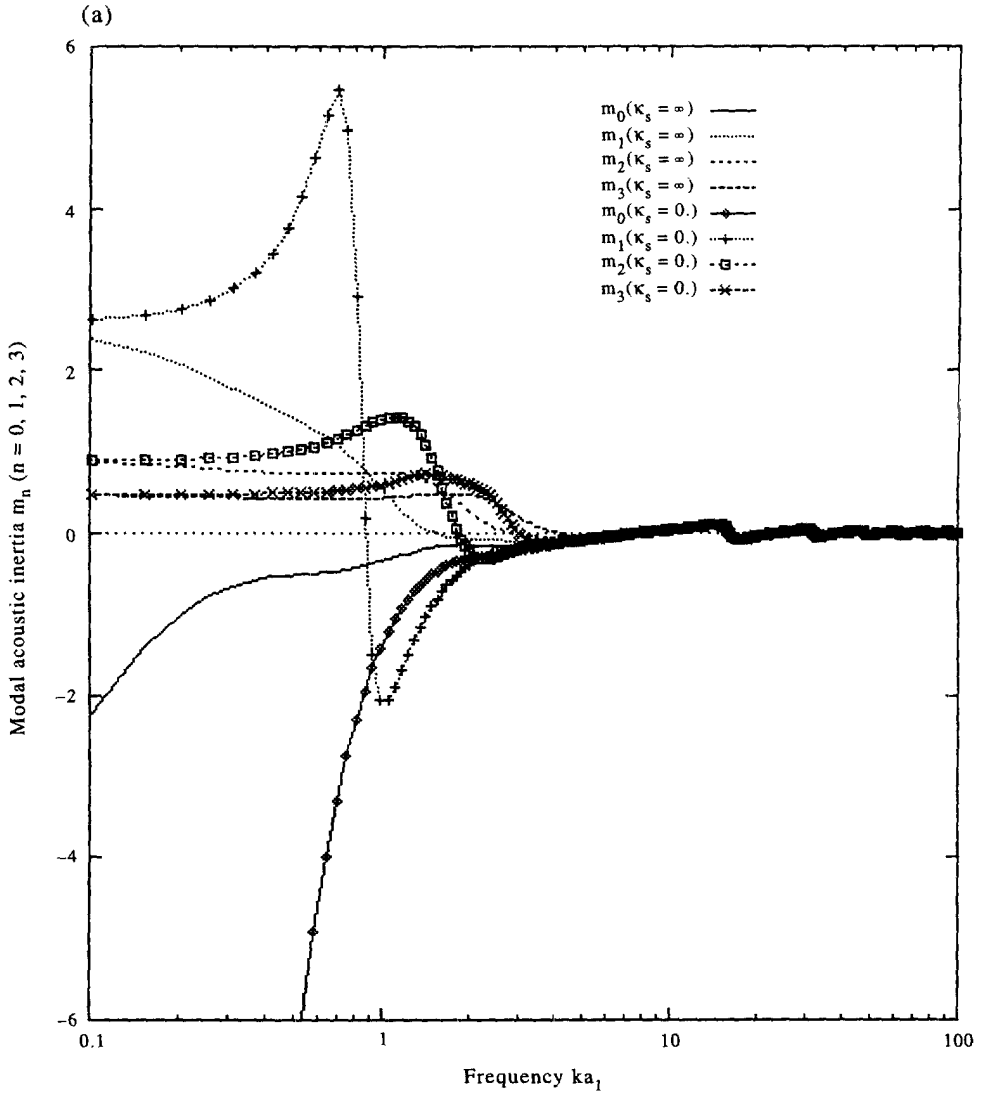

Fig. 4. (a) Effect of interface condition on modal acoustic reactance values (a_2/a_1 = 12 cm/10 cm, $\omega_c a_1/c = 0.56$, other parameters as in Table 1; $m_0 = -180.64@ka_1 = 0.1$); (b) effect of interface condition on modal acoustic resistance values (a_2/a_1 = 12 cm/10 cm, $\omega_c a_1/c = 0.56$, other parameters as in Table 1).

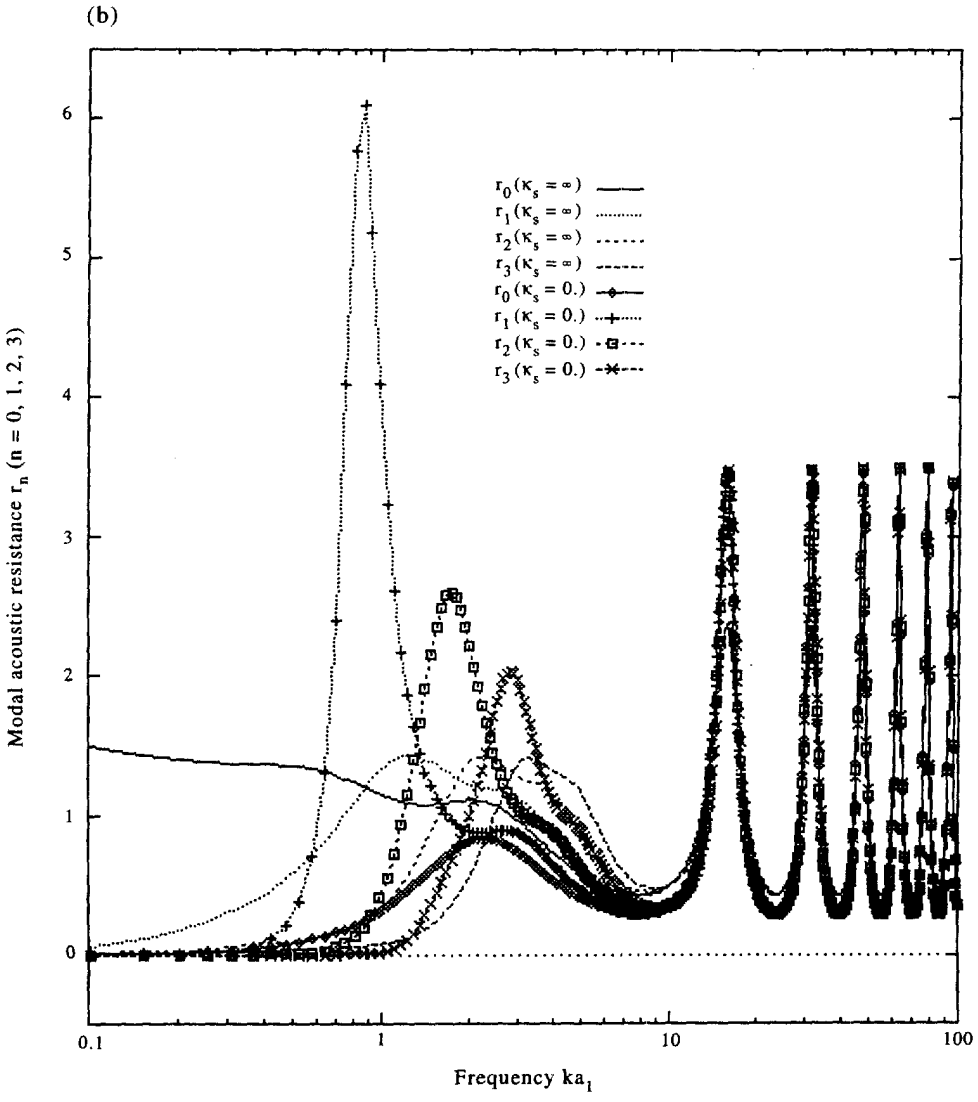

Fig. 4—*Continued.*

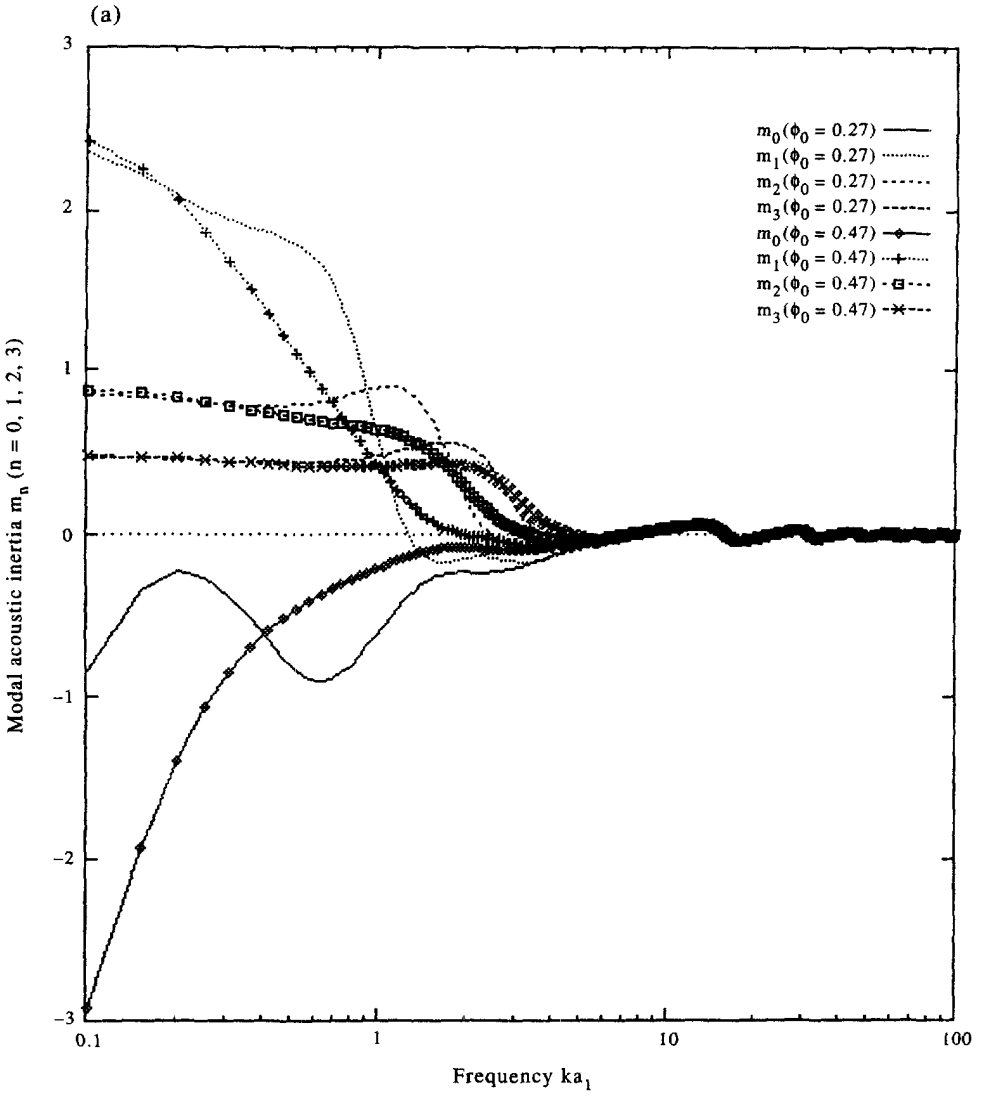

Fig. 5. (a) Influence of porosity on modal acoustic reactance values ($\kappa_s = \infty$, $a_2/a_1 = 12$ cm/10 cm, $\omega_c a_1/c = 0.35, 0.80$, other parameters as in Table 1); (b) influence of porosity on modal acoustic resistance values ($\kappa_s = \infty$, $a_2/a_1 = 12$ cm/10 cm, $\omega_c a_1/c = 0.35, 0.80$, other parameters as in Table 1).

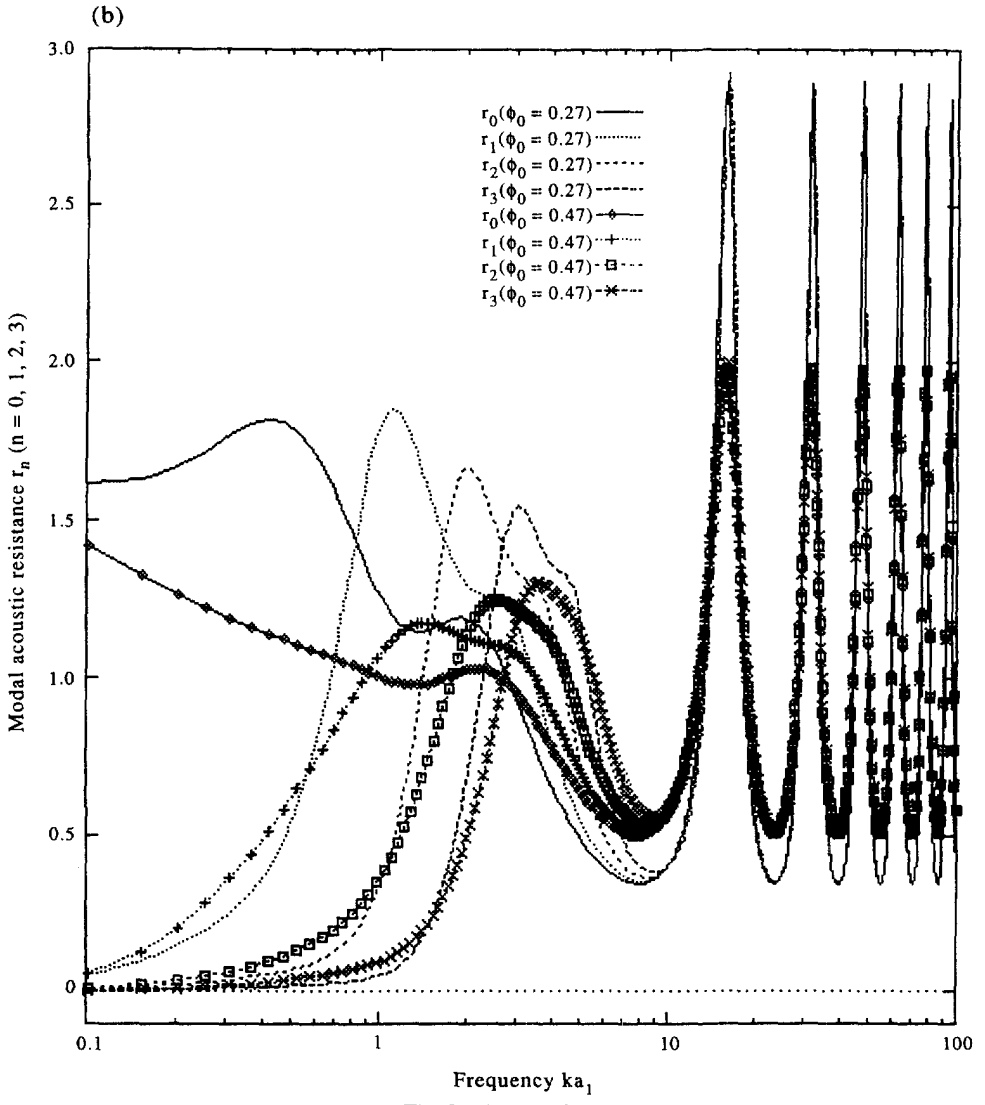

Fig. 5—*Continued.*

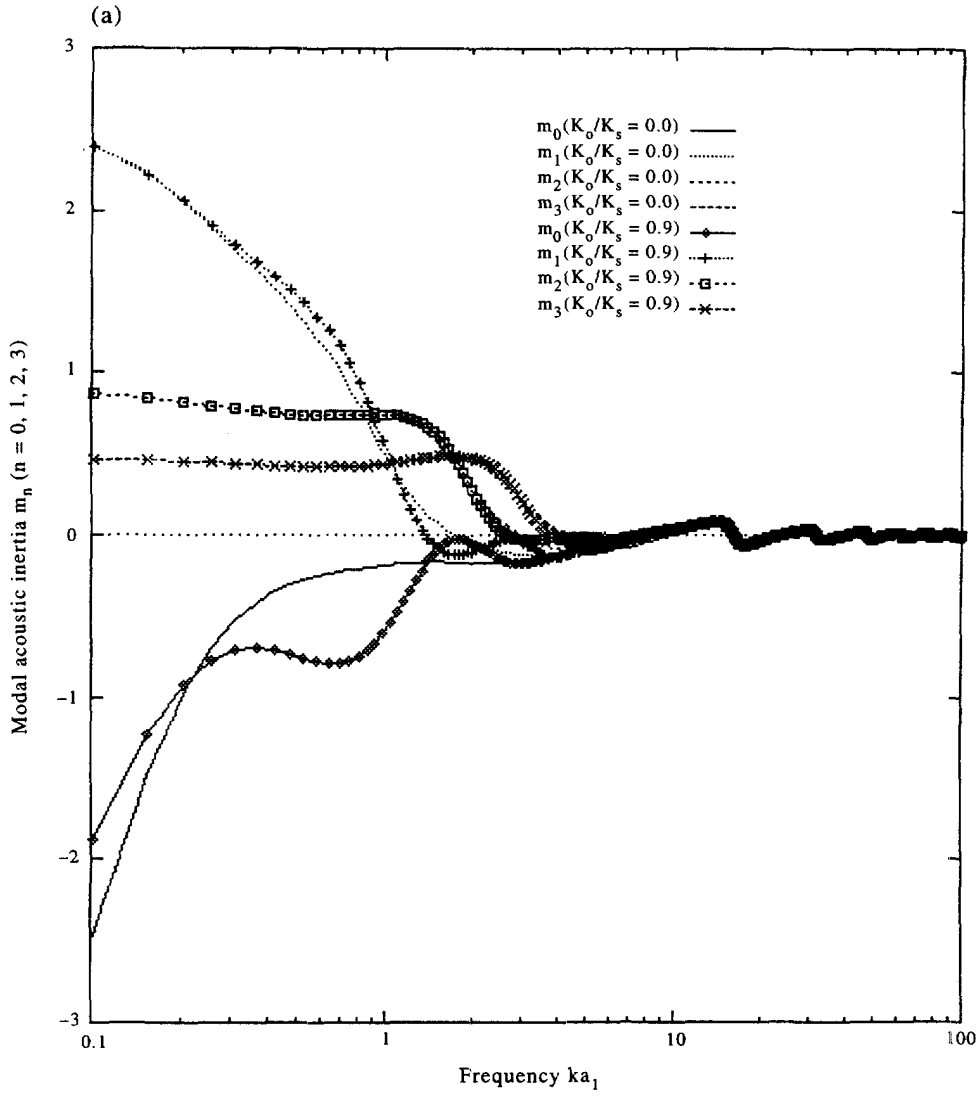

Fig. 6. (a) Effect of frame stiffness on modal acoustic reactance values ($\kappa_s = \infty$, $a_2/a_1 = 12$ cm/10 cm, $\omega_c a_1/c = 0.56$, other parameters as in Table 1); (b) effect of frame stiffness on modal acoustic resistance values ($\kappa_s = \infty$, $a_2/a_1 = 12$ cm/10 cm, $\omega_c a_1/c = 0.56$, other parameters as in Table 1).

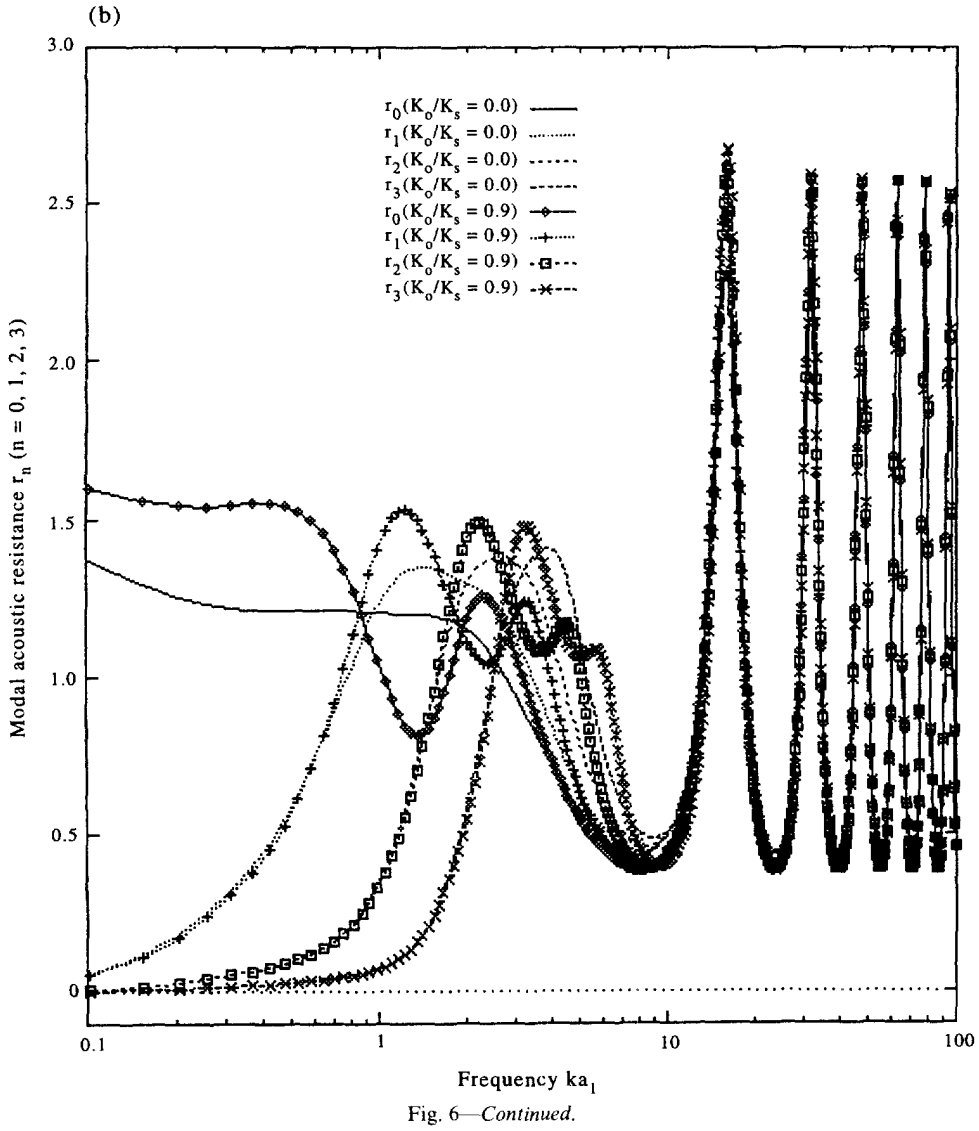

Fig. 6—*Continued.*

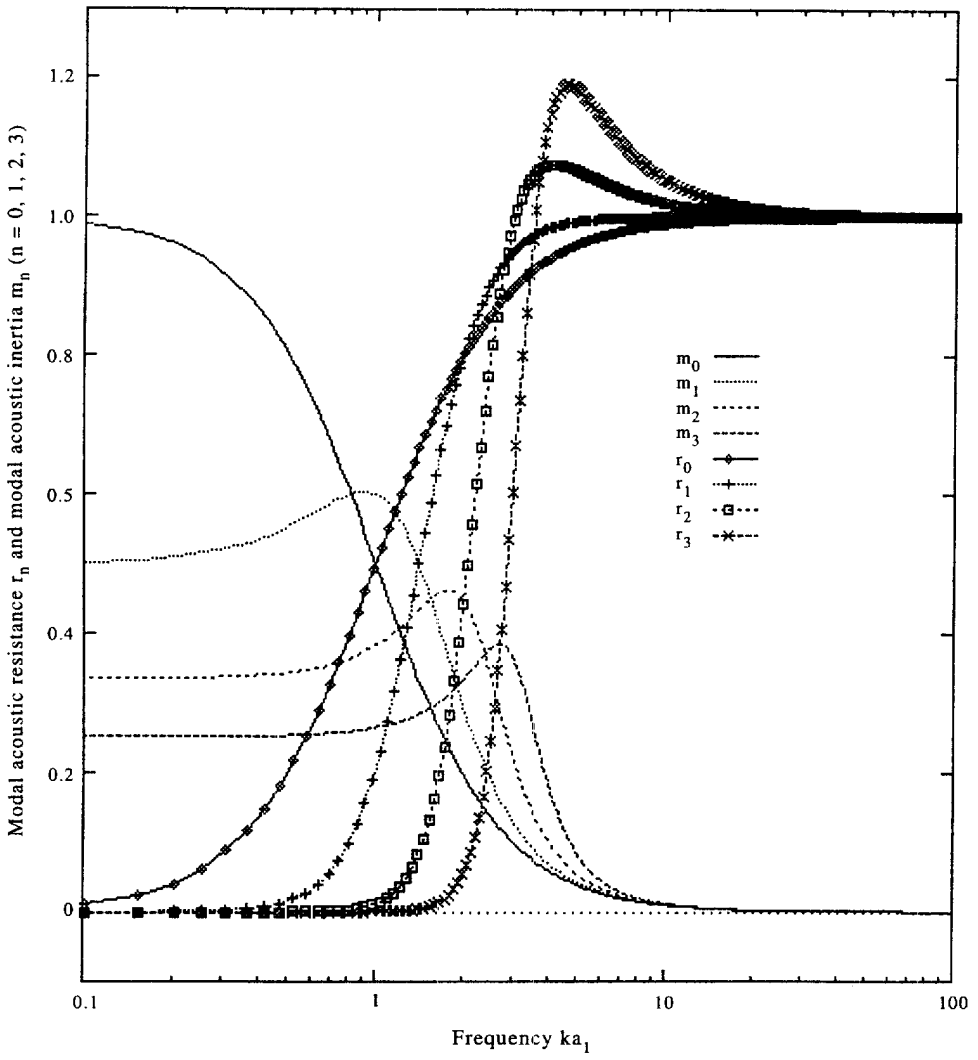

Fig. 7. Modal impedance curves for the "all-fluid" medium approximation ($\kappa_s = \infty$, $a_2/a_1 = 12$ cm/10 cm, $\phi_0 = \alpha = 1$, $K_o = \mu = \eta \approx 0$).

computations. The main outcome is the increase in impedance values as the porosity (tortuosity) decreases (increases). This result is readily conceivable, since as the porosity decreases (tortuosity increases) we anticipate higher force opposing modal vibrations of the spherical surface inside the cavity.

Figures 6a and 6b analyze the effect of frame stiffness for two K_o/K_s ratios, namely $K_o/K_s \cong 0$ and $K_o/K_s = 0.9$. Increasing K_o/K_s at constant porosity corresponds to the existence of increasingly finer pore channels. Therefore here as the frame stiffens, the opposing acoustic force grows which is the precisely expected outcome as displayed in the figures. Finally, to check the validity of our work we consider the "all-fluid" surrounding medium case (Bourbie *et al.*, 1987), i.e., we make the computations for $\phi_0 = \alpha = 1$, and $K_0 = \mu = \eta \cong 0$ as shown in Fig. 7. Evidently, our results reduce to those for modal vibrations of a spherical surface in an ideal infinite acoustic fluid (Junger and Feit, 1972). This simply implies that when there is no impedance mismatch at the interface, we get no wave reflections and hence no wall interference effects exist.

Clearly the overall trends observed, as discussed above, are somewhat anticipated. What is most surprising is the general low frequency behaviour of $n = 0$ (breathing mode) modal resistance curves displayed in the figures. Because acoustic resistance is directly proportional to the radiated power, the notable low frequency values obtained for $r_0(\omega)$ simply implies that the pulsating spherical source (i.e., the expander type transducer) is

expected to be an efficient sound projector even at the low frequency end for the studied configuration.

5. CONCLUSION

Modal acoustic impedance curves have been generated for a spherical radiator in a fluid-filled spherical cavity embedded within an infinite poroelastic medium. These curves are the product of an exact treatment of the fluid-structure interaction which involves utilizing Biot's dynamic model and the appropriate boundary conditions of poroelasticity. Having realized the large number of parameters involved, we present a collection of data merely to illustrate the kinds of results to be expected from some representative and physically realistic choices of values for these parameters. The numerical results reveal the important effects of interface condition, porosity (tortuosity), and frame stiffness on the computed modal acoustic impedance values. They also show that for the studied configuration the pulsating spherical source (i.e., an expander type transducer) is expected to be an efficient sound projector even at the low frequency limit.

The studied configuration is a realistic idealization of a sound projector (transducer) freely suspended in a fluid-filled spherical cavity within a permeable surrounding formation. It is also noted that the presented formulation is equally adequate for situations in which the surrounding formation consists of fibrous materials, as in noise control engineering applications. Therefore, it is hoped that this work may initiate further studies, both theoretical and observational, of acoustics in fluid-saturated elastic porous media. Extension of present effort to determine radiation loading on a spherical source in a fluid-filled cylindrical borehole within a permeable formation, which is of great interest in seismic prospecting applications, is currently underway.

Acknowledgements—The author wishes to sincerely thank professors D. L. Johnson, Amos Nur, J. Dvorkin, P. N. J. Rasolofosaon, J. F. Allard, and M. D. Sharma for valuable and productive consultations on Biot theory of poroelasticity. He is also indebted to a demanding reviewer whose through critique prompted manuscript improvement.

REFERENCES

Abramovitz, M. and Stegun, I. A. (1964) *Handbook of Mathematical Functions*. National Bureau of Standards, Washington, DC.

Achenbach, J. D. (1976) *Wave Propagation in Elastic Solids*. North-Holland, New York.

Allard, J. F. (1993) *Propagation of Sound in Porous Media, Modelling Sound Absorbing Materials*. Elsevier Applied Science, London.

Berryman, J. G. (1980) Confirmation of Biot's Theory. *Applied Physics Letters* **73,** 382–384.

Berryman, J. G. (1982) Elastic waves in fluid-saturated porous media. In *Macroscopic Properties of Disordered Media, Lecture Notes in Physics, 154*, eds R. Burridge *et al*. Springer-Verlag, Berlin, pp. 39–49.

Berryman, J. G. (1985) Scattering by a spherical inhomogeneity in a fluid-saturated porous medium. *Journal of Mathematical Physics* **26,** 1408–1419.

Biot, M. A. (1956a) Theory of propagation of elastic waves in a fluid-saturated porous solid, I: Low-frequency range. *Journal of the Acoustical Society of America* **28,** 168–178.

Biot, M. A. (1956b) Theory of propagation of elastic waves in a fluid-saturated porous solid, I: Low-frequency range. *Journal of the Acoustical Society of America* **28,** 179–191.

Biot, M. A. (1962) Mechanics of deformation and acoustic propagation in porous media. *Journal of Applied Physics* **23,** 1482–1498.

Bourbie, T., Coussy, O. and Zinszner, B. E. (1987) *Acoustics of Porous Media*. Gulf Publishing, Houston.

Cremer, L. W. (1990) *Structure-Borne Sound*, 2nd edn. Springer-Verlag, Berlin.

Deresiewicz, H. and Rice, J. F. (1962) The effect of boundaries on wave propagation in a liquid-filled porous solid, III: Reflection of plane waves at a free boundary. *Bulletin of the Seismological Society of America* **52,** 595–625.

Deresiewicz, H. and Skalak, R. (1963) On uniqueness in dynamic poroelasticity. *Bulletin of the Seismological Society of America* **53,** 783–788.

Gassmann, F. (1951) Uber die elastizitat poroser medien. *Vieteljahrsschrift d Naturforsch. Gesell. Zurich* **96,** 1–23.

Geers, T. L. and Hasheminejad, S. M. (1991) Linear vibration analysis of an ultrasonic cleaning problem. *Journal of Acoustical Society of America* **90,** 3238–3247.

Geertsma, J. and Smit, D. C. (1961) Some aspects of elastic wave propagation in fluid-saturated porous solids. *Geophysics* **26,** 169–181.

Hasheminejad, M. and Geers, T. L. (1992) The accuracy of doubly asymptotic approximations for an acoustic half-space. *Journal of Vibration Acoustics* **114,** 555–563.

Hasheminejad, M. and Geers, T. L. (1993) Modal impedances for two spheres in a thermoviscous fluid. *Journal of the Acoustical Society of America* **94,** 2205–2214.

Johnson, D. L. (1986) Recent developments in the acoustic properties of porous media. In *Frontiers in Physical Acoustics*, Soc. Italiana di Fisica, Bologna, Italy, pp. 255–290.

Johnson, D. L., Koplik, J. and Dashen, R. (1987) Theory of dynamic permeability and tortuosity in fluid-saturated porous media. *Journal of Fluid Mechanics* **76,** 379–402.

Johnson, D. L., Hemmick, D. L. and Kojima, H. (1994a) Probing porous media with first and second sound, I. Dynamic permeability. *Journal of Applied Physics* **76,** 104–114.

Johnson, D. L., Plona, T. J. and Kojima, H. (1994b) Probing porous media with first and second sound, II. Acoustic properties of water-saturated porous media. *Journal of Applied Physics* **76,** 115–125.

Junger, M. C. and Feit, D. (1972) *Sound, Structures, and Their Interaction.* MIT Press, Cambridge.

Kargl, S. G. and Lim, R. (1993) A transition-matrix formulation of scattering in homogeneous, saturated, porous media. *Journal of the Acoustical Society of America* **94,** 1527–1550.

Mei, C. C. and Si, B. I. (1984) Scattering of simple harmonic waves by a circular cavity in a fluid-infiltrated poro-elastic medium. *Wave Motion* **6,** 265–278.

Pao, Y. H. and Mow, C. C. (1973) *Diffraction of Elastic Wave and Dynamic Stress Concentrations.* Crane, Russak, New York.

Plona, T. J. (1980) Observation of the second compressional wave in a porous medium at ultrasonic frequencies. *Applied Physics Letters* **36,** 259–261.

Poterasu, V. F. (1993) Coupled vibrations of a cavity filled with a pulsating fluid in elastic infinite media by the boundary element method. *Computer Methods in Applied Mechanics and Engineering* **106,** 285–296.

Rasolofosaon, P. N. J. (1991) Plane acoustic waves in linear viscoelastic porous media—Energy, particle displacement and physical interpretation. *Journal of the Acoustical Society of America* **89,** 1532–1550.

Thompson, I. J. and Barnett, A. R. (1987) Modified Bessel Functions $I_\nu(z)$ and $K_\nu(z)$ of real order and complex argument, to selected accuracy. *Computer Physics Communications* **47,** 245–257.

White, J. E. (1983) *Underground Sound: Application of Seismic Waves.* Elsevier, Amsterdam.

Winkler, K. W., Liu, H. L. and Johnson, D. L. (1989) Permeability and borehole stonely waves: comparison between experiment and theory. *Geophysics* **54,** 66–75.

Zimmerman, C. (1993) Scattering of plane compressional waves by a spherical inclusion in a poroelastic medium. *Journal of the Acoustical Society of America* **94,** 527–536.